

# Fluctuating Environments Favor Extreme Dormancy Strategies and Penalize Intermediate Ones

Jorge Hidalgo,<sup>1,2</sup> Lorenzo Fant,<sup>3,4</sup> Rafael Rubio de Casas,<sup>5,6</sup> and Miguel A. Muñoz<sup>7,2</sup>

<sup>1</sup>*Departamento de Física, Universidad de Córdoba, 14071 Córdoba, Spain*

<sup>2</sup>*Instituto Carlos I de Física Teórica y Computacional, E-18071, Granada, Spain.*

<sup>3</sup>*Istituto Nazionale di Oceanografia e Geofisica Sperimentale (OGS), Trieste, Italia*

<sup>4</sup>*National Biodiversity Future Centre (NBFC), Palermo Piazza Marina 61, 90133 Palermo, Italy*

<sup>5</sup>*Departamento de Ecología, Universidad de Granada, Granada 18071, Spain*

<sup>6</sup>*Research Unit “Modeling Nature” MNat, Universidad de Granada, Granada 18071, Spain*

<sup>7</sup>*Departamento de Electromagnetismo y Física de la Materia, Universidad de Granada, Granada 18071, Spain*

(Dated: December 8, 2025)

Dormancy is a widespread adaptive strategy that enables biological populations to persist in fluctuating environments. Yet how its evolutionary benefits depend on the temporal structure of environmental variability, and whether dormancy can become systematically maladaptive, remains poorly understood. Here we examine how dormancy interacts with environmental correlation times using a parsimonious delayed-logistic model in which dormant individuals reactivate after a fixed lag while birth rates fluctuate under temporally correlated stochasticity. Numerical simulations and analytical calculations reveal that the joint effect of demographic memory and colored multiplicative noise generates a strongly non-monotonic dependence of fitness on dormancy duration, with three distinct regimes of population performance. Very short dormancy maximizes linear growth but amplifies fluctuations and extinction risk. Very long dormancy buffers environmental variability, substantially increasing mean extinction times despite slower growth. Strikingly, and central to our results, there is a broad band of intermediate dormancy durations that is maladaptive, simultaneously reducing both growth and persistence—an effect that arises generically from the mismatch between delay times and environmental autocorrelation. The predicted bistability between short- and long-dormancy strategies is confirmed in an evolutionary agent-based model, which avoids intermediate lag times and selects for evolutionarily stable extremes. Our results show that dormancy duration is not merely a life-history parameter but an adaptive mechanism tuned to environmental timescales, and that “dangerous middle” dormancy times can be inherently disfavored, with implications for understanding persistence in seed banks, microbial persisters, and cancer cell dormancy. More broadly, this work identifies a general mechanism by which demographic delays interacting with correlated environmental variability generate a non-monotonic fitness landscape that selects for extreme timing strategies, and raises fundamental questions on analyzing delayed, non-Markovian dynamics driven by correlated multiplicative noise near absorbing boundaries.

## I. INTRODUCTION

Dormancy is a widespread phenomenon across the tree of life, occurring in organisms as diverse as bacteria, plants, fungi, insects, and cancer cells [1–3]. Although dormancy takes many forms—such as bacterial persister states, spores, seeds, or quiescent tumor cells—it generally serves the same functional purpose: by delaying growth or reproduction, a fraction of the population can “wait out” unfavorable conditions and enhance long-term survival [4–8].

This strategy is often framed as “dispersal in time”, a temporal analogue of spatial dispersal: whereas classical dispersal spreads offspring across heterogeneous habitats in space, dormancy spreads them across heterogeneous conditions in time, so that lineages can escape adverse conditions along both axes and exploit favorable windows when they arise [6, 9, 10]. From this “space–time” escape perspective, dispersal and dormancy implement complementary adaptive routes that can be tuned by evolution depending on the structure of environmental fluctuations. The evolutionary logic behind dormancy is well supported by laboratory experiments and field stud-

ies. Microbial populations exposed to antibiotic cycles evolve lag-time distributions tuned to the periodicity of the stressor [11, 12], whereas in unpredictable environments they adopt stochastic reactivation strategies that ensure a persistent dormant reservoir [13, 14]. Plant seed banks exhibit similar patterns: predictable seasonal cues favor sharply peaked germination timing, while environments with unpredictable or auto-correlated rainfall select for larger seed banks and broad germination-time distributions [8, 15–21]. Even cancer progression exhibits analogous dynamics: dormant disseminated tumor cells persist for years or decades before reactivating under changing micro-environmental conditions [22, 23].

These examples highlight a fundamental problem: How should organisms tune the duration of dormancy to match the temporal structure of environmental variability? In particular: What is the optimal wake-up time when the environment exhibits a characteristic autocorrelation time? Can maladaptive lag times arise? Can selection favor distinct adaptive peaks separated by sub-optimal strategies? While previous theoretical work has explored the evolution of dormancy under white noise or periodic forcing [5, 24–29], the role of temporal correla-

tions in fluctuating environments remains comparatively understudied, despite abundant empirical evidence that many natural environments exhibit strong autocorrelation (“colored noise”) [26, 30, 31].

In this work, we address these questions using a minimal, yet broadly applicable, delay-logistic model for a population experiencing stochastic environmental conditions with finite correlation time. Individuals reproduce at a rate that fluctuates due to environmental variability and become active only after a fixed dormancy period, introducing a simple form of demographic memory. This framework allows us to isolate how the interaction between temporal correlations and reproductive delay shapes both growth and persistence. Our results reveal a surprisingly rich phenomenology. We show that the interplay of delay and colored noise generates three distinct dynamical regimes. Short delays maximize the linear growth rate but expose the population to strong fluctuations, increasing extinction risk. Long delays strongly suppress variability and enhance persistence at the expense of moderate growth. Most strikingly, intermediate dormancy durations can produce the worst possible outcomes, reducing both growth and resilience. This non-monotonicity arises robustly from the mismatch between the delay window and the environmental autocorrelation structure. We further demonstrate, using an evolutionary agent-based model, that this structure of performance landscapes leads naturally to evolutionary bistability: populations evolve either short or long dormancy times, systematically avoiding the maladaptive intermediate regime. This mirrors empirical observations of bimodal germination strategies in plant seed banks and mixed phenotypic strategies in microbial persisters and in zooplankton propagules [32–36].

Altogether, our study reveals that dormancy duration is an adaptive trait tuned as a function of the timescale of environmental variability, and that correlated environmental noise fundamentally reshapes the fitness landscape of timing strategies. Beyond biological implications, the work exposes open theoretical challenges in understanding delayed, non-Markovian stochastic processes driven by correlated multiplicative noise, especially near absorbing boundaries. Our analysis shows that it is the interplay between demographic delay and environmental correlation—rather than either factor alone—that determines the evolutionary value of dormancy. This interaction generically produces a non-monotonic performance landscape with distinct adaptive peaks.

## II. STOCHASTIC DELAYED-LOGISTIC MODEL FOR POPULATIONS WITH ENVIRONMENTAL NOISE AND DORMANCY

Our model considers a population undergoing logistic growth, governed by a differential equation that incorporates two key mechanisms: (i) environmental stochasticity and (ii) finite maturation time (interpreted as a

reproductive delay) [24] (see upper panel of Figure 1).

In contrast to classical logistic models, reproduction is delayed and influenced by a correlated stochastic environment, while death takes place at a constant rate. In the current, basic formulation of the model, the reproductive delay is a linear function of dormancy.

Consequently, the population density  $x(t)$  evolves according to the following equation:

$$\dot{x}(t) = (b + \sigma \xi_\tau(t)) x(t - \alpha) \left(1 - \frac{x(t)}{K}\right) - d x(t), \quad (1)$$

where  $d$  is the per capita death rate (unless otherwise stated, we set  $d = 1$ ). Following reproduction at time  $t - \alpha$ , the offspring (seed) remains dormant for a fixed duration  $\alpha$  and becomes active at time  $t$ , at which point it can reproduce or die. This leads to a delayed dependence in the birth term [37], which is proportional to the population at the earlier time  $t - \alpha$ . Furthermore, the reproduction rate is modulated by the carrying capacity  $K$  through a logistic saturation term  $1 - x(t)/K$ , evaluated at the time of becoming active. An extended formulation can incorporate  $\alpha$  as a random variable drawn from a probability distribution, thus capturing individual-level variability in dormancy or maturation times:  $x(t - \alpha) \rightarrow \int d\alpha \rho(\alpha) x(t - \alpha)$ , where  $\rho(\alpha)$  represents the distribution of dormancy durations across the population. Although this approach can describe more accurately many situations in nature—including diversification and bet-hedging strategies (see below)—for the moment we focus on treating  $\alpha$  as a fixed control parameter.

Crucially, environmental variability is incorporated into the model through a time-dependent birth rate, which fluctuates as a result of external conditions [38]. Specifically, the intrinsic birth rate is replaced by a stochastic term  $b + \sigma \xi_\tau(t)$ , where  $\xi_\tau(t)$  represents environmental noise.

We represent environmental variability with a dichotomous continuous-time Markov noise (DMN) [39], with states  $\pm 1$  and symmetric transition rate  $\tau^{-1}$ . This modeling choice is mathematically tractable, maintains non-negativity of rates, and encodes alternating “good” and “bad” conditions. As a consequence, the process exhibits a temporal autocorrelation function  $\langle \xi_\tau(t) \xi_\tau(s) \rangle = \exp(-2|t - s|/\tau)$ , with characteristic correlation time  $\tau/2$ . We note that an alternative formulation where environmental variability affects the death rate instead of the birth rate is also possible (see Appendix V D).

The use of DMN ensures that the birth rate remains non-negative as long as  $\sigma \leq b$ , which is essential to prevent nonphysical scenarios in the presence of delay. In fact, if the coefficient multiplying the delayed term becomes negative, the dynamics can reach negative population densities [40, 41]. For this reason, other forms of colored noise—such as Ornstein–Uhlenbeck processes—could induce negative fluctuations in the birth rate, potentially destabilizing the population. Nevertheless, we have verified that the qualitative behavior of the model

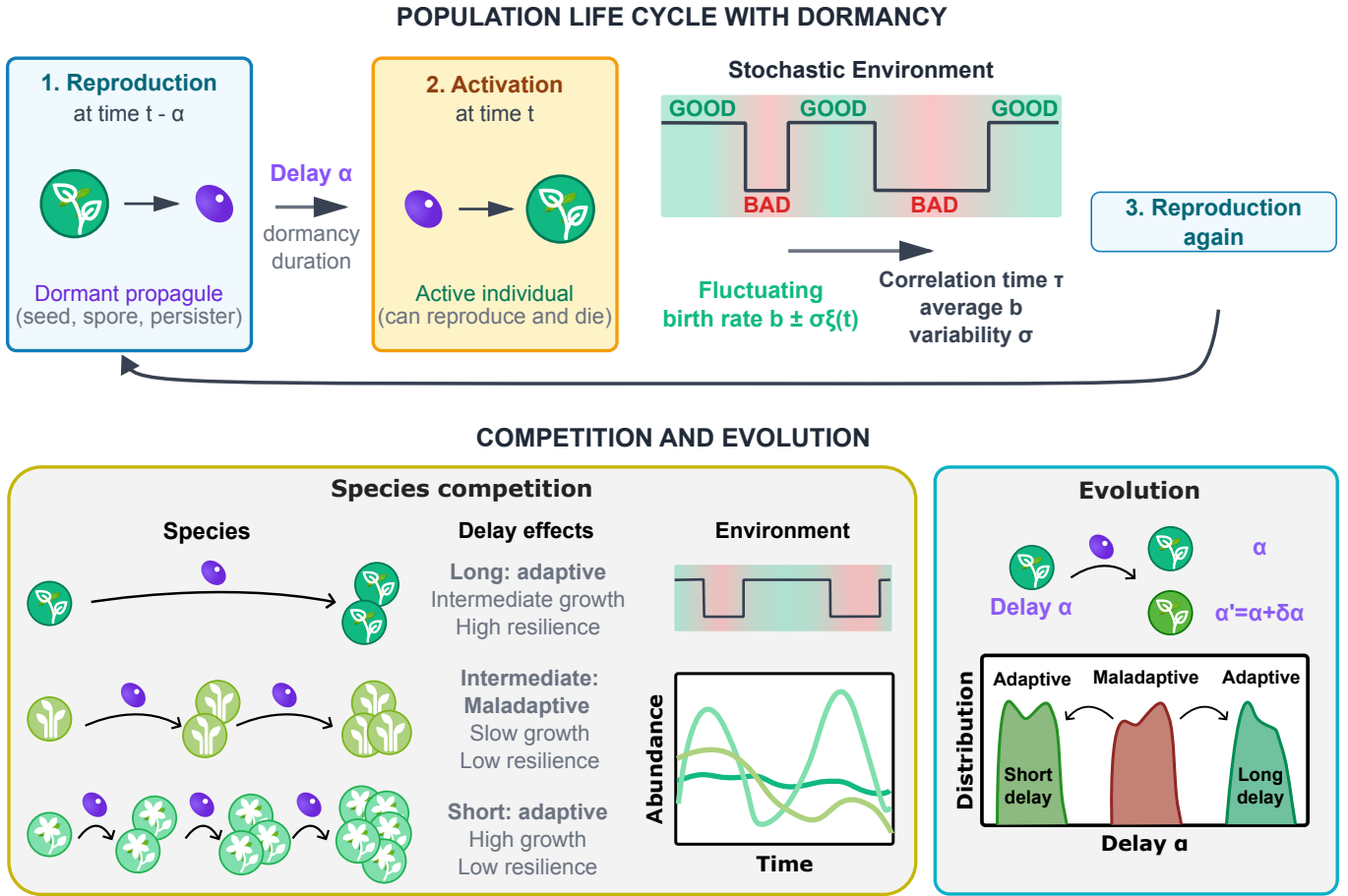


Figure 1. Population life cycle with dormancy in a stochastic environment. Individuals reproduce to produce dormant propagules (e.g., seeds, spores, persister cells) at time  $t - \alpha$ , which remain in a quiescent state for a delay  $\alpha$  before activating into reproductive, mortal individuals at time  $t$ . Active individuals experience alternating good and bad environmental conditions, represented as temporal fluctuations in the birth rate with mean  $b$ , variance  $\sigma$ , and correlation time  $\tau$ . We then use this life-cycle framework to investigate (left) ecological competition among species that differ in dormancy and activation, and (right) evolutionary change in dormancy duration via single mutations that shift the delay from  $\alpha$  to  $\alpha' = \alpha + \delta\alpha$ . In both cases, extreme strategies with either very long or very short delays gain a competitive advantage, whereas intermediate dormancy strategies are maladaptive and are progressively replaced by fitter ones.

remains robust under alternative noise models (see Appendix V C).

It should be noted that the environmental noise term  $\xi_\tau(t)$  could, in principle, be evaluated either at the moment of reproduction  $t - \alpha$ , i.e. when the dormant seed is generated, or at the activation time  $t$ , i.e. when it becomes capable of reproduction and subject to death. In our case, this choice is irrelevant because of the temporal translational invariance of the DMN. However, this distinction may become relevant in extended models with stochastic  $\alpha$  or with multiple interacting populations coupled to the same environmental fluctuations.

This modeling framework enables us to investigate the interplay between dormancy ( $\alpha$ ) and key features of environmental variability—such as its amplitude ( $\sigma$ ) and temporal correlation ( $\tau$ )—and how their interaction shapes the long-term dynamics of populations exposed to fluctuating environments.

We integrate Eq. 1 numerically using an explicit fourth-order Runge-Kutta (RK4) method adapted to handle delay differential equations, following the approach described in [41] (see Appendix V A). As is customary in delayed systems, initial conditions must be specified in the interval  $[-\alpha, 0]$ . In our simulations, we set  $x(t') = x(0)$  for  $t' < 0$ . This choice has no qualitative impact on the long-term dynamics, since the presence of noise rapidly erases the memory of the initial condition. It should be noted that the most interesting phenomenology of the model emerges when the average reproduction rate is just above the critical threshold,  $b \gtrsim d$ , where the interplay between environmental stochasticity and delayed reproduction leads to rich dynamical behavior. In this marginal regime, fluctuations and memory effects can significantly impact population persistence and variability, making the role of dormancy particularly relevant (see Appendix V B). Such a regime, rare in exponential

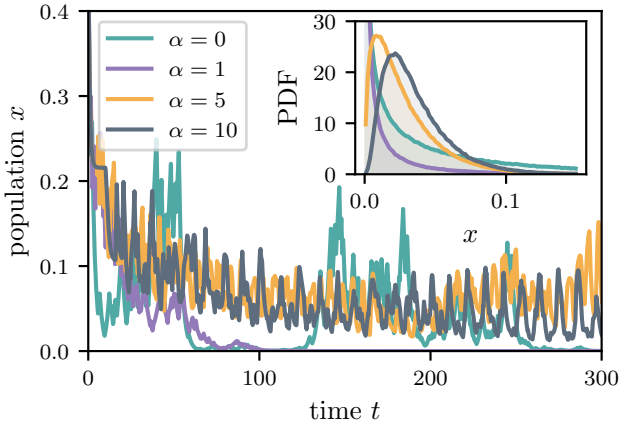


Figure 2. Time series of the population density  $x(t)$  for different values of the dormancy  $\alpha$ , illustrating the effect of delayed reproduction under environmental noise. The inset shows the corresponding stationary probability density functions (PDFs) of  $x(t)$ , highlighting qualitative changes in population variability across dormancy regimes. Parameters:  $b = 1.05$ ,  $\tau = 1$ ,  $\sigma = 0.5$ ,  $d = 1$ ,  $K = 1$ .

growth, is surely suited to describe populations in saturated environments where the overall growth rate is close to zero.

Figure 2 illustrates representative time series of the population density  $x(t)$  for varying dormancy  $\alpha$ , under conditions of pronounced environmental stochasticity. In a nutshell, we identify three regimes: for low dormancy (e.g.,  $\alpha = 0$ ), the population grows rapidly but remains prone to extinction due to strong fluctuations (note that true extinction cannot occur in the absence of demographic noise [42, 43]); at intermediate dormancy values (e.g.,  $\alpha = 1$ ), the system consistently collapses to extinction. For large dormancy values (e.g.,  $\alpha \gtrsim 5$ ), the population stabilizes and oscillates around a steady value, with reduced amplitude in both positive and negative fluctuations.

### A. Mean population diagram

We have explored the phase diagram of the stationary mean population density  $x^*$  as a function of dormancy  $\alpha$  and the noise amplitude  $\sigma$  (see Figure 3).

In the deterministic case ( $\sigma = 0$ ), the population reaches the stationary value  $x^* = (1 - d/b)K$ , which is independent of dormancy. Once environmental fluctuations are introduced ( $\sigma > 0$ ), the mean density becomes strongly dormancy-dependent: the largest values of  $x^*$  occur for vanishing dormancy values ( $\alpha \rightarrow 0$ ), and to a lesser extent for very prolonged dormancy. For intermediate  $\alpha$ , reproduction becomes significantly less effective, producing a pronounced depression in the population level. As  $\sigma$  increases, this depression deepens and broadens, forming a valley of low mean population that

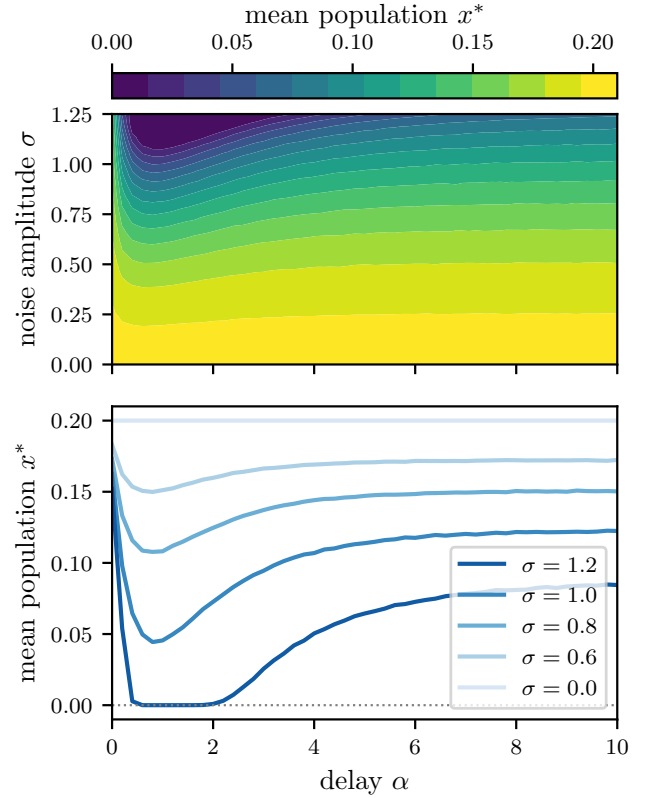


Figure 3. Mean population density  $x^*$  as a function of dormancy  $\alpha$  and noise amplitude  $\sigma$ . Upper panel: heat map of  $x^*$  in the  $(\alpha, \sigma)$  plane. Lower panel: the same data shown as  $x^*$  versus  $\alpha$  for different fixed values of  $\sigma$ , highlighting its non-monotonic behavior. To calculate  $x^*$ , we numerically integrate Eq. 1 up to a burn-in time  $T_{\min}$  to remove transients, compute the time average over the window  $[T_{\min}, T_{\max}]$ , and then average over independent noise realizations. Intermediate dormancy combined with strong noise leads to a marked decrease in population size, reflecting poor timing strategies. Parameters:  $d = 1$ ,  $b = 1.25$ ,  $\tau = 1$ ,  $K = 1$ ,  $T_{\min} = T_{\max}/2$ ,  $T_{\max} = 10^4$ , averages over  $10^3$  realizations.

may eventually drive the system towards extinction.

A qualitatively similar diagram is obtained in the  $(\alpha, \tau)$  plane (not shown) for finite  $\sigma$ , where increasing  $\tau$  has an effect analogous to increasing  $\sigma$ . This will be further clarified in the following section.

### B. Linear growth rate

To gain further insight into the aforementioned phenomenology, we analyze the linearized dynamics by taking the limit  $K \rightarrow \infty$  in Eq. 1. This effectively removes density-dependent saturation effects and isolates the influence of dormancy and environmental variability on the intrinsic growth dynamics:

$$\dot{x}(t) = (b + \sigma \xi_\tau(t)) x(t - \alpha) - d x(t). \quad (2)$$



In this regime, we compute the mean linear growth rate, defined as:

$$G = \lim_{T \rightarrow \infty} \left\langle \frac{\log \left( \frac{x(T)}{x(0)} \right)}{T} \right\rangle, \quad (3)$$

where the average is taken over independent realizations of the environmental noise. In practice, the limit is approximated numerically by choosing a sufficiently large integration time,  $T = T_{\max}$ .

The main panel of Figure 4 shows the mean linear growth rate  $G$  as a function of dormancy  $\alpha$ , for fixed correlation time  $\tau$  and varying noise amplitude  $\sigma$ . The growth rate is always maximal at  $\alpha = 0$ , but its decay with increasing dormancy depends strongly on the level of environmental variability. For small noise amplitudes,  $G(\alpha)$  decreases monotonically. However, beyond a certain threshold in  $\sigma$ , the curve develops a local minimum followed by a local maximum. Notably, for sufficiently large noise amplitudes, this local minimum becomes global, making intermediate dormancy levels the least favorable strategy. This result is consistent with the previous section for finite  $K$ , and depressions in  $G(\alpha)$  at intermediate dormancy durations mirror the valley of low stationary densities reported for  $x^*$  (Figure 3). Finally, in the asymptotic regime of prolonged dormancy,  $\alpha \rightarrow \infty$ , the influence of environmental variability vanishes and  $G(\alpha)$  tends to the deterministic profile ( $\sigma = 0$ ).

The reported behavior becomes even more pronounced as the average birth rate  $b$  approaches the death rate  $d$  (see Appendix VB), indicating that proximity to the extinction threshold magnifies the impact of dormancy times and environmental correlations on  $G$ .

A similar qualitative behavior is observed when keeping  $\sigma$  fixed and increasing the correlation time  $\tau$  (see inset of Figure 4).

### 1. Analytical calculation

We develop a semi-analytical framework to further investigate the influence of each parameter and timescale on  $G(\alpha)$ . The literature provides general approaches to treat either stochastic differential equations with delay and white noise [44], or non-delayed systems subject to colored noise [45], but a unified framework that simultaneously accounts for both delay and time-correlated noise is extremely challenging and, to the best of our knowledge, still lacking. Here, we do not attempt to address this general problem, but rather aim to derive an approximate expression tailored to our model. To this end, let us first analyze the deterministic case ( $\sigma = 0$ ), where the population grows exponentially with a linear growth rate  $G_0$ ,  $x(t) = x(0)e^{G_0 t}$ . Introducing this expression into Eq. 2, one finds that

$$G_0 = be^{-\alpha G_0} - d = b_{\text{eff}} - d, \quad (4)$$

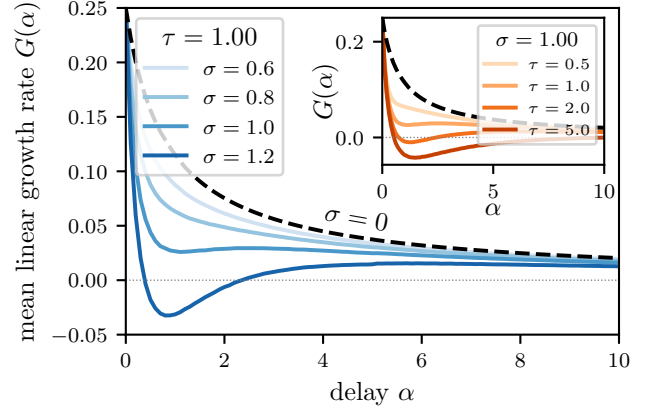


Figure 4. Mean linear growth rate  $G$  as a function of dormancy  $\alpha$ , for different values of the noise amplitude  $\sigma$  (main panel) and correlation time  $\tau$  (inset), in the linearized model (numerical results from simulations). While  $G$  is maximal at  $\alpha = 0$  for all cases, increasing  $\sigma$  or  $\tau$  leads to the emergence of a local minimum at intermediate delays. Parameters:  $d = 1$ ,  $b = 1.25$ ,  $T_{\max} = 10^3$ , averages over  $10^4$  independent realizations.

where we have introduced the effective birth rate  $b_{\text{eff}} = be^{-\alpha G_0}$  for convenience. This implicit equation for  $G_0(\alpha)$  is well known in the literature on delayed population models [40] and must be solved numerically (dashed line in Figure 4).

It is instructive to analyze the behavior of  $G_0(\alpha)$  at small and large delays (i.e., short and long dormancy periods). For short delays, expanding the exponential in Eq. (4) to first order gives  $G_0 \simeq (b-d)(1-\alpha b)$  ( $\alpha \ll b^{-1}$ ). This also shows that the initial decay scale of both  $G_0$  and  $b_{\text{eff}}$  is set by  $b^{-1}$ . For large delays, setting  $y = \alpha G_0$  shows that  $y$  remains bounded and the balance  $be^{-y} \rightarrow d$  is required, hence  $G_0(\alpha) \simeq \ln(b/d)/\alpha$ .

In the presence of fluctuations, we can introduce the ansatz  $x(t) = x(0)e^{-\int_0^t g(s)ds}$  in Eq. 2, where  $g(t)$  is the instantaneous growth rate (note that  $\lim_{t \rightarrow \infty} \langle g(t) \rangle = G$ ). We then obtain an equation for  $g(t)$  that must be solved self-consistently:

$$g(t) = (b + \sigma \xi_\tau(t)) e^{-\int_{t-\alpha}^t ds g(s)} - d. \quad (5)$$

The integral can be estimated in two asymptotic limits. For **small delays** ( $\alpha \ll b^{-1}$ ), we approximate the integral by evaluating it at time  $t$ ,  $\int_{t-\alpha}^t g(s) ds \simeq \alpha g(t)$ . Then we write  $g(t) = G_0 + \sigma g_1(t)$  and Taylor expand  $e^{-\alpha \sigma g_1(t)}$  to linear order in  $\alpha$ . We further assume that the noise amplitude  $\sigma$  is small and discard all mixed terms of order  $\sigma^2 \alpha$ . Many terms cancel, yielding an explicit equation for  $g_1(t)$ :

$$g_1(t) = \frac{b_{\text{eff}}/b}{1 + b_{\text{eff}}\alpha} \xi_\tau(t). \quad (6)$$

This result can be introduced in Eq. 5 to compute the

mean linear growth rate  $G$  for small delays:

$$\begin{aligned} G_{\text{small}} &= \left\langle (b + \sigma \xi_\tau(t)) e^{-G_0 \alpha} \left( 1 - \sigma \frac{b_{\text{eff}}/b}{1 + b_{\text{eff}} \alpha} \int_{t-\alpha}^t \xi_\tau(s) ds \right) \right\rangle \\ &= G_0 - \sigma^2 \frac{(b_{\text{eff}}/b)^2}{1 + b_{\text{eff}} \alpha} \int_{t-\alpha}^t \langle \xi_\tau(t) \xi_\tau(s) \rangle ds \\ &= G_0 - \frac{1}{2} \sigma^2 \tau \frac{(b_{\text{eff}}/b)^2}{1 + b_{\text{eff}} \alpha} \left( 1 - e^{-2\alpha/\tau} \right). \end{aligned} \quad (7)$$

where we have used  $\langle \xi_\tau(t) \xi_\tau(s) \rangle = e^{-2|t-s|/\tau}$ .

On the other hand, for **large delays** ( $\alpha \gg b^{-1}$ ), the integral can be replaced by its mean value,  $\int_{t-\alpha}^t g(s) ds \simeq \alpha G_{\text{large}}$ , and taking the average in Eq. 5 yields an implicit equation for  $G_{\text{large}}$  that coincides with Eq. 4. Therefore,

$$G_{\text{large}} = G_0, \quad (8)$$

as indeed is observed in Figure 4.

We finally introduce a heuristic expression that interpolates between the two regimes,  $G(\alpha) = f(\alpha) G_{\text{small}} + (1 - f(\alpha)) G_{\text{large}}$ , where  $f(\alpha)$  is an interpolation function, e.g.  $f(\alpha) = (1 + b\alpha)^{-1}$ ; other choices for this function yield similar performance and do not significantly affect the forthcoming results. Substituting the expressions, we obtain:

$$G = G_0 - \frac{1}{2} \sigma^2 \tau \frac{(b_{\text{eff}}/b)^2}{(1 + b_{\text{eff}} \alpha)(1 + b\alpha)} \left( 1 - e^{-2\alpha/\tau} \right). \quad (9)$$

We have assessed the validity of this approximation in Figure 5 (solid line), comparing it with numerical simulations for increasing values of  $\sigma$  at fixed  $\tau$  (upper panel), and increasing  $\tau$  at fixed  $\sigma$  (lower panel). Overall, the agreement is good: it captures the qualitative dynamics and the locations of the local extrema. This provides a semi-analytical expression that captures the dependence of the growth rate on the model parameters.

The noise-induced correction in Eq. 9 exhibits a single peak (see Figure 5) from competition between the decreasing term  $\frac{(b_{\text{eff}}(\alpha)/b)^2}{(1 + \alpha b_{\text{eff}}(\alpha))(1 + b\alpha)}$  and the increasing factor  $(1 - e^{-2\alpha/\tau})$ . Each factor acts on its own scale: the former decays over  $b^{-1}$  (via  $b_{\text{eff}}$  and the denominators), while the latter grows over the environmental correlation time  $\tau/2$ . Although we cannot provide a closed-form expression for the peak location—marking the time of worst performance—its scale is set by the shorter limiting timescale,  $\alpha_* \sim \min\{\tau/2, b^{-1}\}$ .

### C. Extinction times

We now explore the resilience of the population to external perturbations by analyzing how dormancy duration impacts the mean extinction time. It is important to note that in order to observe true extinction ( $x = 0$ ), demographic fluctuations must be included in Eq. 1. In the absence of demographic noise, the absorbing state cannot be reached in finite time [42].

To overcome this limitation, we adopt the following standard approach: we introduce an artificial absorbing

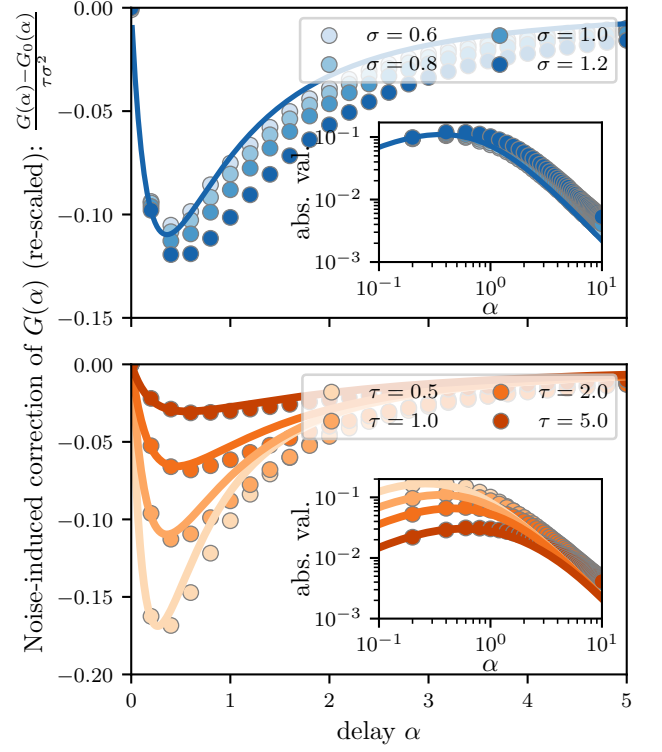


Figure 5. Noise-induced correction to the mean linear growth rate as a function of dormancy  $\alpha$ , rescaled by the factor  $\tau \sigma^2$ . Solid lines correspond to the approximation given in Eq. 9, while points denote numerical simulation results. Top panel: fixed correlation time  $\tau = 1$  and varying noise amplitude  $\sigma$ . Bottom panel: fixed  $\sigma = 1$  and varying  $\tau$ . Insets show the same data (in absolute value) on log-log scale, highlighting the asymptotic decay at large values of  $\alpha$ . Parameters:  $d = 1$ ,  $b = 1.25$ .

boundary at  $x = 1/N$ , effectively mimicking the population density corresponding to a single individual in a finite population of size  $N$ . Starting from a given initial history—here  $x(t) = K/2$  for  $t \in [-\alpha, 0]$ , with results robust to other smooth histories—we compute the mean first-passage time  $\bar{T}$  to this boundary, which we use as a proxy for the mean extinction time. This procedure yields results consistent with more elaborate demographic simulations while remaining computationally efficient [46, 47], and shows no strong dependence on  $N$ .

Figure 6 shows the dependence of  $\bar{T}$  on the effective system size  $N$  for different values of dormancy  $\alpha$ . In all cases,  $\bar{T}$  increases with  $N$ . Interestingly, prolonged dormancy consistently leads to longer mean extinction times. For the set of parameters chosen here, distinct scaling regimes emerge depending on  $\alpha$ :  $\bar{T}$  grows relatively slowly with  $N$  when dormancy is short (i.e., sub-linearly), indicating limited resilience. In contrast, for larger values of dormancy, the population becomes more stable, and  $\bar{T}$  increases more rapidly with  $N$ . This behavior is consistent with the trends observed in Figure 2

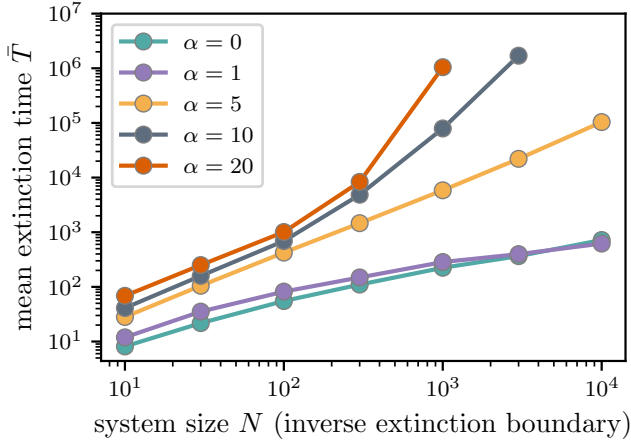


Figure 6. Mean extinction time  $\bar{T}$  (measured as the time to reach the absorbing boundary  $x = 1/N$ ) as a function of system size  $N$ , for different values of the dormancy  $\alpha$ . Parameters:  $d = 1$ ,  $b = 1.05$ ,  $\tau = 1$ ,  $\sigma = 0.5$ ,  $K = 1$ . Each point represents an average over  $10^3$  realizations.

(where we use the same parameter values to facilitate comparison), where large delays suppress both positive and negative fluctuations, thereby reducing extinction risk. This result highlights the stabilizing effect of dormancy under environmental variability.

So far, we have analyzed two key indicators of population performance: the ability to grow under unbounded conditions, captured by the mean linear growth rate  $G$  (in the limit  $K \rightarrow \infty$ ), and the ability to persist over time, measured by the mean extinction time  $\bar{T}$  (with an absorbing boundary at  $x = N^{-1}$ ). In Figure 7, we make an explicit comparison between these two quantities, both by fixing the correlation time  $\tau$  and varying the noise amplitude  $\sigma$  (upper panel), and by fixing  $\sigma$  and varying  $\tau$  (lower panel). Each point corresponds to a different value of dormancy  $\alpha$ .

As expected, the system faces a trade-off: short dormancy maximizes growth ( $G$ ) but results in shorter extinction times ( $\bar{T}$ ), whereas prolonged dormancy promotes resilience at the cost of slower growth. These differences become more pronounced under strong ( $\sigma$  large) or persistent ( $\tau$  large) environmental fluctuations. Interestingly, both panels reveal a non-monotonic behavior: the curve bends backward for intermediate values of  $\alpha$ , simultaneously lowering  $G$  and  $\bar{T}$ . These regimes correspond to the least favorable strategies identified in previous sections.

### III. AGENT-BASED, EVOLUTIONARY DYNAMICS

The results developed so far—both deterministic and stochastic—show that demographic delay interacting with temporally correlated environmental variability gen-

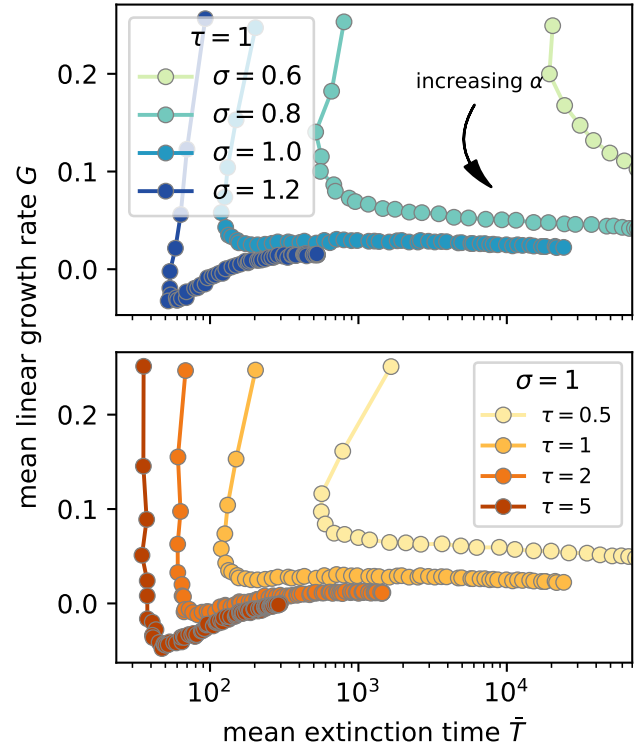


Figure 7. Trade-off between mean linear growth rate  $G$  and mean extinction time  $\bar{T}$  for different values of the dormancy  $\alpha$ . Each curve corresponds to a different level of environmental variability. Parameters:  $d = 1$ ,  $b = 1.25$ . To calculate  $G$ , we set  $K \rightarrow \infty$  and  $T_{\max} = 10^3$ , and to calculate  $\bar{T}$  we set  $K = 1$ ,  $N = 10^3$ . In both cases, we average over  $10^3$  realizations.

erates a fitness landscape with two adaptive peaks and a maladaptive intermediate region. However, these analyses quantify growth and persistence, not evolutionary success. In real biological systems, natural selection operates on populations composed of individuals with heritable variation, demographic stochasticity, and finite lifetimes. Whether the non-monotonic structure identified above truly translates into evolutionary dynamics is therefore not guaranteed.

To test whether the predicted bistability represents a genuine evolutionary mechanism, we developed an explicit agent-based model in which dormancy behavior is an evolving trait subject to mutation and natural selection (see lower panel of Figure 1). The ecological setting matches the stochastic environment studied in Section II: resources fluctuate between “good” and “bad” states according to a dichotomous Markov process with correlation time  $\tau$ . Agents consume resources, reproduce proportionally to intake, and generate propagules that remain inactive until they establish. Importantly, each individual carries an inheritable activation rate  $\alpha$ , which governs the probability per unit time that a propagule becomes active. While this formulation introduces natural variability in dormancy duration, its role here is not

to modify the phenomenology of delay, but to allow dormancy strategies to evolve in a biologically realistic manner. Mortality affects only active agents, enabling dormant propagules to form a persistent reservoir analogous to seed banks or microbial persisters. All ecological and evolutionary events are simulated in continuous time using a Gillespie algorithm [48], ensuring full demographic and environmental stochasticity.

Despite these additional sources of variability and the lack of any imposed fixed delay, the evolutionary outcomes closely mirror the predictions derived from the delayed-logistic framework. As shown in Figure 7, populations starting with low values of  $\alpha$  evolve toward a stable short-dormancy strategy, while those starting with large  $\alpha$  converge to a stable long-dormancy strategy. Crucially, populations initiated with intermediate  $\alpha$  do not remain there. Instead, stochastic evolutionary trajectories drift away from the maladaptive region, ultimately reaching one of the two adaptive strategies. This confirms that the performance valleys and peaks identified in Sections II and II.C represent true evolutionary features, not artifacts of fixed-delay assumptions or idealized population-level models.

The emergence of evolutionary bistability in this fully stochastic model parallels empirical observations of timing strategies in nature, such as those found in microbial persisters, plant seed banks, and other systems where populations diversify into fast-activating and long-dormant phenotypes. These results demonstrate that the dual adaptive strategies revealed by our analysis are robust to demographic noise, architecture of dormancy, and details of trait inheritance, reinforcing the view that the interaction between demographic memory and environmental temporal structure fundamentally shapes the evolution of dormancy.

#### IV. CONCLUSIONS AND DISCUSSION

We have investigated how dormancy duration shapes population performance in environments characterized by temporal correlations. Using a minimal delayed-logistic model with stochastic birth rates, we showed that delayed reproduction and colored environmental noise interact in a highly nontrivial way, producing distinct dynamical regimes and revealing a general principle: the adaptive value of dormancy depends critically on the relationship between the delay time and the environmental autocorrelation timescale.

Our analysis demonstrates that reproductive delay plays a dual, tightly balanced role. Very short dormancy maximizes the linear growth rate, exploiting favorable conditions but amplifying susceptibility to rare downturns. Conversely, prolonged dormancy buffers environmental variability, enhancing resilience and substantially increasing extinction times even when growth is slow. Most strikingly, our work reveals the emergence of maladaptive intermediate dormancy durations—lag

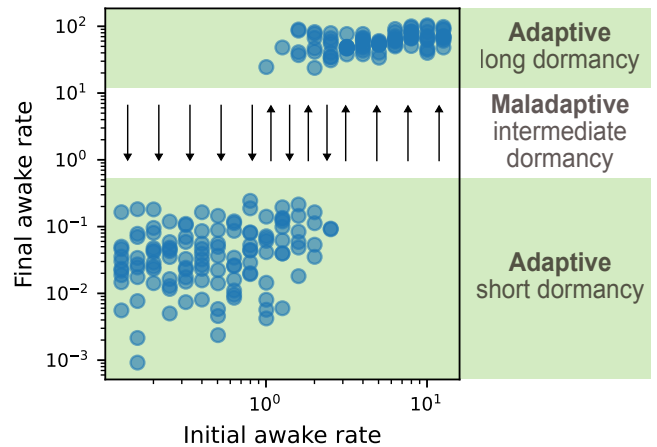


Figure 8. Evolutionary validation of the predicted bistable dormancy strategies. Final population-mean awake rates  $\alpha$  are plotted against their initial values across independent evolutionary simulations. The population consistently evolves toward one of two adaptive attractors: a short-dormancy strategy or a long-dormancy strategy, while avoiding intermediate values. Populations initiated in the maladaptive region never remain there; instead, natural selection drives them toward one of the two fitness peaks predicted by the delayed-logistic analysis. Parameter values:  $\mu = 100$ ,  $\sigma = 90$ ,  $d = 0.1$ ,  $\nu = 0.01$  and  $\tau = 4$ ; simulation time is  $2 \times 10^5$ .

times that simultaneously reduce both growth and persistence below the values of both adaptive phases. This non-monotonicity arises robustly from the mismatch between demographic memory and the temporal structure of environmental variability, and it appears across numerical simulations, analytical approximations, and evolutionary models.

These findings show that the fitness landscape of dormancy is not smooth but organized around a bistable structure, with two adaptive peaks separated by a broad maladaptive valley of intermediate dormancy times. This bistability is confirmed in a fully stochastic, evolutionary agent-based model: populations consistently evolve toward either short or long dormancy durations, avoiding the intermediate region. Such evolutionary outcomes mirror empirical patterns in diverse biological systems, including bimodal germination strategies in plant seed banks—where mixed populations of fast-germinating individuals and a persistent dormant reservoir coexist [49–55]—and phenotypic diversification into active and dormant subpopulations in microbes. In cancer, analogous transitions between quiescent and proliferative states suggest that both extremes can contribute to the survival and spread of tumors. Our results can provide a theoretical framework to understand why intermediate, partially active states where cells are neither fully dormant nor fully proliferative, are particularly susceptible to therapeutic intervention [22, 23, 56]. Further research should expand on this to clarify why intermediate or transitional dormancy stages are maladaptive and to what extent this



can be manipulated by exogenous factors.

More broadly, our results position dormancy not as a passive life-history constraint but as an adaptive timing mechanism tuned to environmental timescales. The dependence of fitness on the interaction between demographic delay and environmental correlation implies that organisms should evolve lag times matched to the predictability of their environment. This framework therefore contributes to a unified ecological and evolutionary understanding of dormancy across biological domains.

Overall, this study provides a minimal but powerful theoretical foundation for understanding how temporal environmental structure shapes adaptive dormancy strategies. It opens the door to exploring evolutionarily stable distributions of lag times, multimodal bet-hedging strategies, and the ecological and physiological constraints that may shape the observed diversity of dormancy behaviors in nature.

Beyond its biological implications, the present work underscores fundamental theoretical challenges. The model highlights the complexity of delayed, non-Markovian stochastic processes driven by correlated multiplicative noise near absorbing boundaries, an area where rigorous analytical tools remain limited. Our approximate analytical treatment provides initial insight, but future progress will require developing general methods to handle delay kernels, correlated noise, and extinction dynamics in a unified framework.

## ACKNOWLEDGMENTS

We thank J. Grilli for his very insightful comments and suggestions. We are also extremely grateful to A. Maritan, S. Suweis, S. Azaele, M. Sireci and J.M. Camacho for enjoyable past collaborations on closely related topics. This work has been supported by Grants Nos. PID2022-143099OB-I00 and PID2023-149174NB-I00 financed by the Spanish Ministry and Agencia Estatal de Investigación MICIU/AEI/10.13039/501100011033 and European Regional Development Funds (ERDF). Thanks to the European Union Next-Generation EU (PIANO NAZIONALE DI RIPRESA E RESILIENZA (PNRR) – MISSIONE 4 COMPONENTE 2, “Dalla ricerca all’impresa” INVESTIMENTO 1.4 – D.D. 1034 17/06/2022, CN00000033).

## V. APPENDICES

### A. Numerical integration

We use an explicit Runge-Kutta method of fourth order adapted to handle delay differential equations, fol-

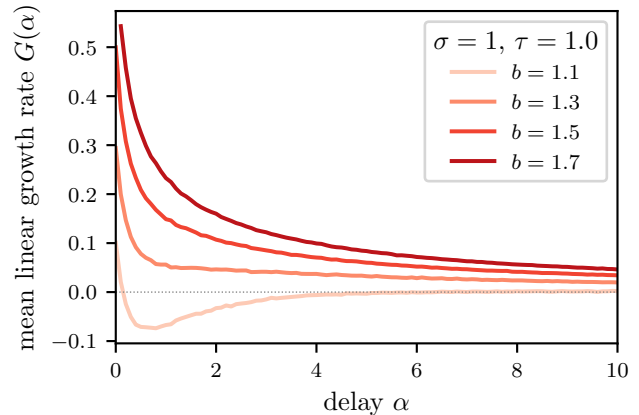


Figure 9. Mean linear growth rate  $G$  as a function of the reproductive delay  $\alpha$  for different mean birth rates  $b$  (simulations with the model presented in the main text). The non-monotonic behaviour of  $G(\alpha)$  and the emergence of least favorable strategies become more evident when  $b \rightarrow d$ , approaching the extinction threshold. Parameters:  $d = 1$ ,  $\sigma = 1$ ,  $\tau = 1$ ,  $T_{\max} = 10^3$ , averages over  $10^2$  independent realizations.

lowing the procedure outlined in [41]. The key idea is to discretize time with a fixed step  $\Delta t$  and store the past history of the solution in a buffer or ring array, enabling efficient evaluation of the delayed term  $x(t - \alpha)$  by interpolation. In our simulations, we typically use time steps  $\Delta t \lesssim 0.01$ , which ensures numerical stability and accuracy across the range of delays and noise intensities considered.

It is worth mentioning that, for the linearized dynamics, we performed the numerical integration using a change of variables; in particular, for numerical convenience, we integrate the dynamics in logarithmic space, defining  $z = \log(x)$ , so that Eq. 2 becomes:

$$\dot{z} = (b + \sigma \xi_\tau(t)) e^{z(t-\alpha)-z(t)} - d. \quad (10)$$

No additional stochastic calculus (e.g., Itô corrections) is required, as the noise has finite correlation time.

### B. Dependence on the average birth rate $b$

Figure 9 shows the dependence of the mean linear growth rate  $G(\alpha)$  on the reproductive delay  $\alpha$  for different values of the mean birth rate  $b$ . As expected, the overall growth rate  $G$  decreases as  $b$  approaches the critical threshold  $d$ . More interestingly, the emergence of least favorable strategies—signaled by local minima in  $G(\alpha)$ —becomes more pronounced in this marginal regime. This reinforces the idea that proximity to the extinction threshold amplifies the influence of reproductive delay and environmental structure on population performance.

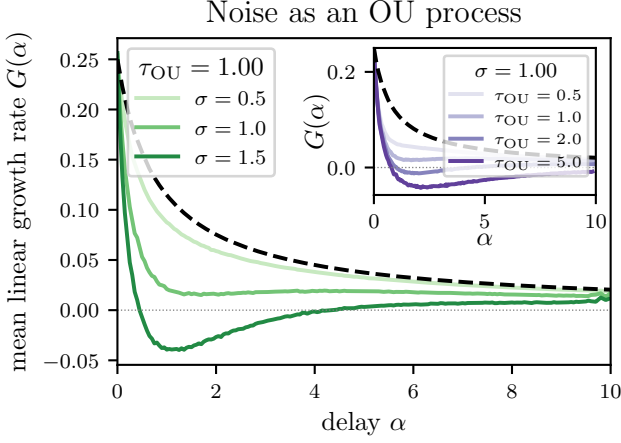


Figure 10. Mean linear growth rate  $G$  as a function of the reproductive delay  $\alpha$  when the birth rate is driven by an Ornstein–Uhlenbeck process and rectified as  $\max(0, b' + \sigma \xi_{\text{OU}}(t))$ . Main panel: dependence on the noise amplitude  $\sigma$  at fixed  $\tau_{\text{OU}}$ ; inset: dependence on the correlation time  $\tau_{\text{OU}}$  at fixed  $\sigma$  (simulation results). In all cases, the same phenomenology emerges as for dichotomic noise (see main text). To enable a fair comparison,  $b'$  is chosen so that the time-average of the birth rate equals  $b$ . Parameters:  $d = 1$ ,  $b = 1.25$ ;  $b'(\sigma=0.5) = 1.249$ ,  $b'(\sigma=1) = 1.194$ ,  $b'(\sigma=1.5) = 1.035$ ;  $T_{\text{max}} = 10^3$ ; averages over  $10^3$  independent realizations.

### C. Environment modeled as an Ornstein-Uhlenbeck process

The environment can be also modeled as an Ornstein-Uhlenbeck process:

$$\dot{\xi}_{\text{OU}}(t) = -\frac{1}{\tau_{\text{OU}}} \xi_{\text{OU}} + \sqrt{\frac{2}{\tau_{\text{OU}}}} \eta(t), \quad (11)$$

where  $\eta(t)$  is a zero mean, delta-correlated white Gaussian noise. In this case, the environment has zero mean and characteristic time of temporal correlation  $\tau_{\text{OU}}$  [57].

As discussed in the main text, care is needed when integrating regimes where the effective birth rate can become negative: even the simple delay equation  $\dot{x} = -x(t - \alpha)$  has the (a priori stable) fixed point  $x^* = 0$  losing stability beyond a critical delay, and the same mechanism appears in models with delayed birth and death terms [40, 41]. For this reason, in simulations we enforce a non-negative birth rate to avoid unphysical destabilization induced by delay.

To address this issue, we model the birth rate as  $\max(0, b' + \sigma \xi_{\text{OU}}(t))$  (i.e., no offspring are produced when the environmental variable falls below a threshold). However, when  $\sigma \gtrsim b'$ , the time-averaged birth rate  $b$  differs from  $b'$ . To enable fair comparisons across  $\sigma$ , we therefore choose  $b' = b'(\sigma)$  so that the average birth rate is fixed to  $b$ . Results are shown in Figure 10. The same phenomenology as in the case studied in the

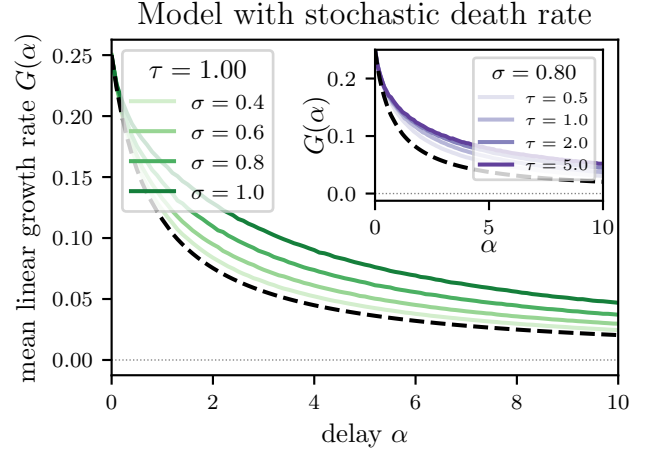


Figure 11. Mean linear growth rate  $G$  as a function of the reproductive delay  $\alpha$ , for different values of the noise amplitude  $\sigma$  (main panel) and correlation time  $\tau$  (inset), in the linearized model with stochastic death rate (simulation results). In contrast to the case with noise in the birth rate, here  $G(\alpha)$  decreases monotonically with increasing delay, regardless of  $\sigma$  or  $\tau$ . This highlights the crucial role of the coupling between noise and delay in generating non-monotonic behaviors. Parameters:  $d = 1$ ,  $b = 1.25$ ,  $d = 1$ ,  $T_{\text{max}} = 10^3$ , averages over  $10^3$  independent realizations.

main text (with dichotomic noise) emerges, highlighting the robustness of the observed behavior.

### D. Environmental variability in the death rate

In the main text, we considered environmental variability acting on the birth process. Here, we explore an alternative scenario in which fluctuations instead affect the death rate. Since dormancy modulates only the birth term, the delay remains confined to reproduction, and the stochastic differential equation becomes:

$$\dot{x}(t) = b x(t - \alpha) \left(1 - \frac{x(t)}{K}\right) - (d + \sigma \xi_{\tau}(t)) x(t). \quad (12)$$

Figure 11 shows the results of integrating this model in the linear regime ( $K \rightarrow \infty$ ), using dichotomous Markov noise (DMN). In contrast to the case where fluctuations act on the birth rate, here the mean linear growth rate  $G(\alpha)$  decays monotonically with the reproductive delay  $\alpha$ , without developing any local extrema. This indicates that the emergence of least favorable strategies—i.e., intermediate values of  $\alpha$  that simultaneously reduce growth and persistence—is not a generic consequence of delay under noise. Instead, such regimes result specifically from the direct coupling between reproductive delay and environmental variability, which is absent when noise acts solely on the instantaneous death rate.

- [1] J. T. Lennon and S. E. Jones, Microbial seed banks: the ecological and evolutionary implications of dormancy, *Nature reviews microbiology* **9**, 119 (2011).
- [2] C. C. Baskin and J. M. Baskin, *Seeds: ecology, biogeography, and evolution of dormancy and germination* (Academic press, 2000).
- [3] D. L. Denlinger, Regulation of diapause, *Annual review of entomology* **47**, 93 (2002).
- [4] D. Cohen, Optimizing reproduction in a randomly varying environment, *Journal of theoretical biology* **12**, 119 (1966).
- [5] M. Bulmer, Delayed germination of seeds: Cohen's model revisited, *Theoretical Population Biology* **26**, 367 (1984).
- [6] D. Cohen and S. A. Levin, The interaction between dispersal and dormancy strategies in varying and heterogeneous environments, in *Mathematical Topics in Population Biology, Morphogenesis and Neurosciences: Proceedings of an International Symposium held in Kyoto, November 10–15, 1985* (Springer, 1987) pp. 110–122.
- [7] Y. Iwasa and S. A. Levin, The timing of life history events, *Journal of Theoretical Biology* **172**, 33 (1995).
- [8] J. T. Lennon, F. den Hollander, M. Wilke-Berenguer, and J. Blath, Principles of seed banks and the emergence of complexity from dormancy, *Nature Communications* **12**, 4807 (2021).
- [9] J. R. Gremer and D. L. Venable, Bet hedging in desert winter annual plants: optimal germination strategies in a variable environment, *Ecology Letters* **17**, 380 (2014).
- [10] R. Rubio de Casas, K. Donohue, D. L. Venable, and P.-O. Cheptou, Gene-flow through space and time: dispersal, dormancy and adaptation to changing environments, *Evolutionary Ecology* **29**, 813 (2015).
- [11] O. Fridman, A. Goldberg, I. Ronin, N. Shoshitaishvili, and N. Q. Balaban, Optimization of lag time underlies antibiotic tolerance in evolved bacterial populations, *Nature* **513**, 418 (2014).
- [12] J. Camacho Mateu, M. Sireci, and M. A. Muñoz, Phenotypic-dependent variability and the emergence of tolerance in bacterial populations, *PLoS computational biology* **17**, e1009417 (2021).
- [13] E. Kussell and S. Leibler, Phenotypic diversity, population growth, and information in fluctuating environments, *Science* **309**, 2075 (2005).
- [14] T. M. Norman, N. D. Lord, J. Paulsson, and R. Losick, Stochastic switching of cell fate in microbes, *Annual review of microbiology* **69**, 381 (2015).
- [15] W. R. Shoemaker and J. T. Lennon, Evolution with a seed bank: the population genetic consequences of microbial dormancy, *Evolutionary applications* **11**, 60 (2018).
- [16] M. Rees, Evolutionary ecology of seed dormancy and seed size, *Philosophical Transactions of the Royal Society of London. Series B: Biological Sciences* **351**, 1299 (1996).
- [17] D. L. Venable and L. Lawlor, Delayed germination and dispersal in desert annuals: escape in space and time, *Oecologia* **46**, 272 (1980).
- [18] C. G. Willis, C. C. Baskin, J. M. Baskin, J. R. Auld, D. L. Venable, J. Cavender-Bares, K. Donohue, R. Rubio de Casas, and NGW Group, The evolution of seed dormancy: environmental cues, evolutionary hubs, and diversification of the seed plants, *New Phytologist* **203**, 300 (2014).
- [19] K. Donohue, R. Rubio de Casas, L. Burghardt, K. Kovach, and C. G. Willis, Germination, postgermination adaptation, and species ecological ranges, *Annual Review of Ecology, Evolution, and Systematics* **41**, 293 (2010).
- [20] R. Rubio de Casas, C. G. Willis, W. D. Pearse, C. C. Baskin, J. M. Baskin, and J. Cavender-Bares, Global biogeography of seed dormancy is determined by seasonality and seed size: a case study in the legumes, *New Phytologist* **214**, 1527 (2017).
- [21] A. Măgălie, D. A. Schwartz, J. T. Lennon, and J. S. Weitz, Optimal dormancy strategies in fluctuating environments given delays in phenotypic switching, *Journal of theoretical biology* **561**, 111413 (2023).
- [22] J. A. Aguirre-Ghiso, Models, mechanisms and clinical evidence for cancer dormancy, *Nature Reviews Cancer* **7**, 834 (2007).
- [23] T. G. Phan and P. I. Croucher, The dormant cancer cell life cycle, *Nature Reviews Cancer* **20**, 398 (2020).
- [24] G. E. Hutchinson *et al.*, Circular causal systems in ecology, *Ann. NY Acad. Sci* **50**, 221 (1948).
- [25] Y. Himeoka and N. Mitarai, When to wake up? the optimal waking-up strategies for starvation-induced persistence, *PLoS computational biology* **17**, e1008655 (2021).
- [26] S. Tuljapurkar, *Population dynamics in variable environments*, Vol. 85 (Springer Science & Business Media, 2013).
- [27] S. Moreno-Gámez, D. J. Kiviet, C. Vulin, S. Schlegel, K. Schlegel, G. S. van Doorn, and M. Ackermann, Wide lag time distributions break a trade-off between reproduction and survival in bacteria, *Proceedings of the National Academy of Sciences* **117**, 18729 (2020).
- [28] E. Şimşek and M. Kim, Power-law tail in lag time distribution underlies bacterial persistence, *Proceedings of the National Academy of Sciences* **116**, 17635 (2019).
- [29] J. Baranyi, Stochastic modelling of bacterial lag phase, *International journal of food microbiology* **73**, 203 (2002).
- [30] R. C. Lewontin and D. Cohen, On population growth in a randomly varying environment, *Proceedings of the National Academy of sciences* **62**, 1056 (1969).
- [31] S. Tuljapurkar, Delayed reproduction and fitness in variable environments., *Proceedings of the National Academy of Sciences* **87**, 1139 (1990).
- [32] W. C. Ratcliff and R. F. Denison, Bacterial persistence and bet hedging in *sinorhizobium meliloti*, *Communicative & integrative biology* **4**, 98 (2011).
- [33] Z. Wang, J. M. Baskin, C. C. Baskin, G. Liu, X. Ye, X. Yang, and Z. Huang, Soil salinity regulates spatial-temporal heterogeneity of seed germination and seedbank persistence of an annual diaspore-trimorphic halophyte in northern china, *BMC Plant Biology* **24**, 604 (2024).
- [34] D. Cao, C. C. Baskin, J. M. Baskin, F. Yang, and Z. Huang, Comparison of germination and seed bank dynamics of dimorphic seeds of the cold desert halophyte *suaeda corniculata* subsp. *mongolica*, *Annals of Botany* **110**, 1545 (2012).
- [35] A. Berkvens, P. Chauhan, and F. J. Bruggeman, Integrative biology of persister cell formation: molecular circuitry, phenotypic diversification and fitness effects, *Journal of the Royal Society Interface* **19**, 20220129 (2022).
- [36] C. E. Cáceres and A. J. Tessier, How long to rest: the

- ecology of optimal dormancy and environmental constraint, *Ecology* **84**, 1189 (2003).
- [37] L. F. Lafuerza and R. Toral, Stochastic description of delayed systems, *Philosophical Transactions of the Royal Society A: Mathematical, Physical and Engineering Sciences* **371**, 20120458 (2013).
  - [38] D. A. Vasseur and P. Yodzis, The color of environmental noise, *Ecology* **85**, 1146 (2004).
  - [39] I. Bena, Dichotomous markov noise: exact results for out-of-equilibrium systems, *International Journal of Modern Physics B* **20**, 2825 (2006).
  - [40] Y. Kuang, *Delay differential equations* (Academic press New York, 1993).
  - [41] H. Wernecke, B. Sándor, and C. Gros, Chaos in time delay systems, an educational review, *Physics Reports* **824**, 1 (2019).
  - [42] M. A. Muñoz, Nature of different types of absorbing states, *Physical Review E* **57**, 1377 (1998).
  - [43] W. Genovese and M. A. Muñoz, Recent results on multiplicative noise, *Physical Review E* **60**, 69 (1999).
  - [44] T. Frank, Delay fokker-planck equations, perturbation theory, and data analysis for nonlinear stochastic systems with time delays, *Physical Review E* **71**, 031106 (2005).
  - [45] P. Jung and P. Hänggi, Dynamical systems: a unified colored-noise approximation, *Physical review A* **35**, 4464 (1987).
  - [46] T. Spanio, J. Hidalgo, and M. A. Muñoz, Impact of environmental colored noise in single-species population dynamics, *Physical Review E* **96**, 042301 (2017).
  - [47] J. Hidalgo, S. Suweis, and A. Maritan, Species coexistence in a neutral dynamics with environmental noise, *Journal of theoretical biology* **413**, 1 (2017).
  - [48] D. T. Gillespie, A general method for numerically simulating the stochastic time evolution of coupled chemical reactions, *Journal of computational physics* **22**, 403 (1976).
  - [49] J.-W. Veening, W. K. Smits, and O. P. Kuipers, Bistability, epigenetics, and bet-hedging in bacteria, *Annual Review of Microbiology* **62**, 193 (2008), PMID: 18537474.
  - [50] D. Z. Childs, C. Metcalf, and M. Rees, Evolutionary bet-hedging in the real world: empirical evidence and challenges revealed by plants, *Proceedings of the Royal Society B: Biological Sciences* **277**, 3055 (2010).
  - [51] E. Rotem, A. Loinger, I. Ronin, I. Levin-Reisman, C. Gabay, N. Shores, O. Biham, and N. Q. Balaban, Regulation of phenotypic variability by a threshold-based mechanism underlies bacterial persistence, *Proceedings of the National Academy of Sciences* **107**, 12541 (2010).
  - [52] C. E. Tarnita, A. Washburne, R. Martínez-García, A. E. Sgro, and S. A. Levin, Fitness tradeoffs between spores and nonaggregating cells can explain the coexistence of diverse genotypes in cellular slime molds, *Proceedings of the National Academy of Sciences* **112**, 2776 (2015).
  - [53] R. Martínez-García and C. E. Tarnita, Seasonality can induce coexistence of multiple bet-hedging strategies in *Dictyostelium discoideum* via storage effect, *Journal of Theoretical Biology* **426**, 104 (2017).
  - [54] M. Loreau, M. Barbier, E. Filotas, D. Gravel, F. Isbell, S. J. Miller, J. M. Montoya, S. Wang, R. Aussenac, R. Germain, *et al.*, Biodiversity as insurance: from concept to measurement and application, *Biological Reviews* **96**, 2333 (2021).
  - [55] P. Villa Martín, M. A. Muñoz, and S. Pigolotti, Bet-hedging strategies in expanding populations, *PLoS computational biology* **15**, e1006529 (2019).
  - [56] Y. Wang, L. Liu, X. Zhang, T. Liang, and X. Bai, Cancer dormancy and metabolism: From molecular insights to translational opportunities, *Cancer Letters* **635**, 218097 (2025).
  - [57] C. Gardiner, *Stochastic Methods: A Handbook for the Natural and Social Sciences*, Springer Series in Synergetics (Springer, 2009).